Dynamically Cell Separating Thermo-functional Biointerfaces with Densely Packed Polymer Brushes

Kenichi Nagase[1], Ayaka Kimura[1,2], Tatsuya Shimizu[1], Katsuhisa Matsuura[1]
*Masayuki Yamato[1], Naoya Takeda[2], and Teruo Okano[1]**

1. Institute of Advanced Biomedical Engineering and Science, Tokyo Women's Medical University (TWIns), 8-1 Kawadacho, Shinjuku, Tokyo 162-8666, Japan.
2. Department of Life Science and Medical Bioscience, School of Advanced Science and Engineering, Waseda University (TWIns), 2-2 Wakamatsucho, Shinjuku, Tokyo 162-8480, Japan.

*Corresponding author: (Phone) +81-3-5367-9945 Ext. 6201; (Fax) +81-3-3359-6046; (E-mail) tokano@abmes.twmu.ac.jp

Keywords: Intelligent materials, Temperature-responsive polymer, Poly(*N*-isopropylacrylamide), Polymer brush, Cell separation, Regenerative medicine.

Short title for page headings: Thermo-responsive Polymer Brush for Cell Separation

Abstract

Poly(*N*-isopropylacrylamide)(PIPAAm) brush with various brush lengths grafted glass surfaces were prepared as a cell separating intelligent interface through a surface-initiated atom transfer radical polymerization (ATRP) with a CuCl/Me_6TREN catalytic system and α-chloro-*p*-xylene as a free initiator in 2-propanol at 25 °C for 16 h. Characterization of the prepared surface was performed by X-ray photoelectron spectroscopy (XPS), attenuated total reflection Fourier transform infrared spectroscope (ATR/FT-IR), and gel permeation chromatography (GPC) measurement of PIPAAm in ATRP reaction solution for estimating brush length. Phase transition behavior of PIPAAm in four cell culture mediums was also investigated by measuring the temperature-dependent turbidities. Prepared PIPAAm brush surfaces as a cell separating intelligent interfaces were characterized by observing the adhesion and detachment behavior of four types of human cells; human umbilical vein endothelial cells (HUVEC), normal human dermal fibroblasts (NHDF), human aortic smooth muscle cells (SMC), and human skeletal muscle myoblast cells (HSMM). PIPAAm brush surface with a moderate brush length exhibited a proper cells adhesion and detachment behavior, while short-brush-surface scarcely detached cells and long-brush-surfaces scarcely adhered cells. PIPAAm brush with a moderate brush length exhibited the different cell detachment rates among individual cell types. Utilizing the different cells detachment properties, a mixture of green fluorescent protein (GFP) expressing HUVEC (GFP-HUVEC) and HSMM was separated. After being allowed to adhere on the surfaces at 37 °C for 24 h, the adhered cells on the surfaces were incubated at 20 °C. In the initial period of incubation at 20 °C, GFP-HUVEC was released from the surface due to its prompt detachment property, and in the subsequent period of incubation, HSMM gradually detached themselves from the surface. These results indicated that precisely designed PIPAAm brush functioned as an intelligent cell separating interface by utilizing the intrinsic cell detachment properties of individual cells.

Introduction

With progress in biomedical technologies, regenerative medicine that reproduces the lost functions of the tissue and organs has been becoming one of the promising therapies for patients. Especially, cells based regenerative therapy has been progressing rapidly, and a number of clinical trials have already started.[1-3] Cell therapy using direct injection shows an enormous potential for recovering the functions of the tissues and organs.[1] However, the poor survival of injected cells reduces the expected therapeutic effect.[4, 5] Thus, tissue engineering for constructing implantable tissue in vitro has attracted attention as the second generation of cell therapy. Tissue engineering using biodegradable scaffolds has been widely utilized for constructing tissues,[6] and some of the bio-engineered tissues implanted to patients successfully.[7] In contrast, our laboratory has developed a novel tissue engineering approach without any scaffolds, which is called "cell sheet technology".[8, 9] In this approach, thermo-responsive cell culture dishes, prepared by attaching poly(*N*-isopropylacrylamide) (PIPAAm)[10] on tissue culture polystyrene, were used for preparing an artificial tissue consisting of monolayer cells. At 37 °C, cells adhere and proliferate on the PIPAAm modified cell culture substrate, because PIPAAm is hydrophobic due to its dehydration. Then, with reducing temperature to 20 °C, the cultured cells detached themselves as a contiguous cell sheet from the surfaces, due to the hydration and swelling of grafted PIPAAm on the culture surfaces.[9, 11] _ENREF_11 Fabricated cell sheets have been utilized for various types of tissue engineering and regenerative medicines.[12-15] Especially, in several types of tissues, clinical trials using cell sheets have already started.[2, 3] In this way, the fabrication of transplantable tissue in vitro is a key concept in current regenerative medicine.

In the fabrication of the tissues, an effective cell separation and purification technology that can provides an adequate purity, yield, and function after separation have been needed for preparing and constructing tissues, because the purity of cells or individual cell contents in co-cultured cells is important for fabricating functional tissues.[16, 17] To date, various types of cell separation methods have been developed such as field-flow fractionation (FFF),[18, 19] affinity adsorption,[20, 21] and flow sortings.[22, 23] Especially, fluorescence-activated cell sorting (FACS) and magnetic cell sorting (MACS) are

widely used as precise cell separation methods.[22-24] However, these cell separation methods require the modification of cell surfaces with fluorescent antibody or magnetic particles, leading to a serious problem upon the transplantation of separated cells to human body. Thus, a cell separation method that requires no modification on the surface of cell is preferable for utilizing separated cells for transplantation.

With investigating new cell separating tools, our laboratory has paid attention to PIPAAm modified surfaces as a cell separating material. In the preparations of various types of cell sheets, various types of cells are found to exhibit various cell adhesion and detachment properties on PIPAAm grafted surfaces. Utilizing cells' intrinsic adhesive and detachment properties, targeted cells are expected to be obtained by an external temperature change. In addition, recovered cells have already been proved safe for transplantation, because cells sheets fabricated on a PIPAAm modified surface have already been used to clinical applications without any problems.[2, 3]

Additionally, a surface-initiated atom transfer radical polymerization (ATRP) was utilized for preparing cell separating surface. Several attachment methods of PIPAAm on substrate have been established, such as electron-beam radiation,[8, 25] radical polymerization,[26] reversible addition-fragmentation chain transfer radical (RAFT) polymerization,[27] ATRP,[28] and polymer casting. Among them, ATRP is expected to be a good candidate for preparing cell separating surfaces, because ATRP provides a densely packed PIPAAm brush structure (more than 0.1 chains/nm^2),[29] leading to reduction in the amount of undetachable cells and protein on substrate.[30] Also, brush length can be precisely controlled by changing feed monomer concentration or polymerization period in ATRP.[29, 31]

In the present study, PIPAAm brush grafted surfaces with various brush lengths were prepared by a surface-initiated ATRP. Temperature-dependent adhesion and detachment properties of human cells were observed for investigating the possibility of the surface as a cell separating material.

Experimental

Materials

N-isopropylacrylamide (IPAAm) was kindly provided by Kohjin (Tokyo, Japan) and recrystallized from *n*-hexane. CuCl and α-chloro-*p*-xylene were purchased from Wako Pure Chemicals (Osaka). Tris(2-aminoethyl)amine (TREN) was purchased from Acros Organics (Pittsburg, PA, USA). Formaldehyde, formic acid, and sodium hydroxide were purchased from Wako Pure Chemicals. Tris(2-*N*,*N*-dimethylaminoethyl)amine (Me_6TREN) was synthesized from TREN, according to the previous reports.[32] Glass coverslips (24 x 50 mm, 0.2 mm in thickness) were purchased from Matsunami Glass (Osaka). Ethylenediamine-*N*, *N*, *N'*, *N'*-tetraacetic acid disodium salt dehydrate (EDTA·2Na) were purchased from Wako Pure Chemicals. ((Chloromethyl)phenylethyl) trimethoxysilane (mixed *m, p* isomers) as an ATRP initiator was obtained from Gelest (Morrisville, PA). 2-Propanol (HPLC grade), dichloromethane, and toluene (dehydrate) were purchased from Wako Pure Chemicals. Tissue culture polystyrene dishes (TCPS) (Falcon 3002) were obtained from BD Bioscience (Billerica, MA). Cells and cell culture mediums were obtained from Takara Bio (Shiga). Green fluorescent protein (GFP) expressing human umbilical vein endothelial cells (GFP-HUVEC) was obtained from Angio-Proteomie (Boston, MA). Water used in this study was Milli-Q water prepared by an ultrapure water purification system (Synthesis A10) (Millipore, Billerica, MA) unless otherwise mentioned.

Preparation of ATRP Initiator Immobilized Cover Glass slips

Glass coverslips with a silane layer comprising of 2-(*m/p*-chloromethylphenyl) ethyltrimethoxysilane, an ATRP initiator, was prepared as shown in the first step in Fig 1. Glass coverslips were cleaned by oxygen plasma irradiation (the irradiation intensity: 400 W, oxygen pressure: 0.1 mmHg) for 180 s in a plasma dry cleaner (PX-1000) (March Plasma Systems, Concord, CA). Immediately after the plasma oxidation, these glass coverslips were placed in a separable flask (500 mL), which was humidified at 60% relative humidity for 2 h. Toluene solution of ATRP initiator

(46.3 mmol/L in 700 mL) was poured into the separable flask, of which solution was stirred for 16 h. The ATRP initiator immobilized glass coverslips were rinsed with toluene and acetone, and dried in a vacuum oven at 110 °C.

Surface modification of glass surface with PIPAAm by ATRP

PIPAAm grafted surfaces with various chain lengths were prepared by modulating the initial monomer concentration of IPAAm in surface initiated-ATRP as shown in the second step in Fig. 1. Typical preparation procedure was as follows: 25.9 g (275 mmol), 42.7 g (481 mmol), and 51.9 g (550 mmol) of IPAAm were dissolved in 450 mL of 2-propanol, resulting in 500 mmol L^{-1}, 875 mmol L^{-1} and 1000 mmol L^{-1} IPAAm solutions, respectively. The solution was deoxygenated by argon gas bubbling for 30 min. CuCl (295 mg, 3 mmol) and Me_6TREN (765 mg, 3.3 mmol) were added under a argon atmosphere, and the solution was stirred for 20 min to obtain a CuCl/Me_6TREN catalyst system. Both monomer solution in a beaker and the silane-modified coverslips in a 1000 mL separable flask were placed separately into a glove box, which was purged with dry argon gas by repeated vacuum and argon flush (three times). The monomer solution was then poured into the flask containing the glass cover slips, followed by adding α-chloro-*p*-xylene (39.48 μL, 0.3 mmol) to the reaction solution. The ATRP reaction proceeded for 16 h at 25 °C under continuous stirring on a magnetic stirrer (AMG-S) (ASH, Chiba). PIPAAm grafted glass cover slips were washed with acetone, methanol, 50 mmol/L EDTA solution, and finally water, and the modified coverslips were dried in a high vacuum oven at 50 °C for 5 h. The reaction solution after polymerization was dialyzed against Milli-Q water using dialysis membrane [Spectra/Por standard regenerated cellulose dialysis membrane, Molecular Weight Cut Off (MWCO): 1000] (Spectrum Laboratories, Rancho Dominguez, CA) for 1 week with daily water changed, and the polymer was recovered by freeze-drying. Number-average molecular weights and polydispersity index (PDI) values of the polymers were determined by a GPC system (the columns: TSKgel SuperAW2500, TSKgel SuperAW3000, and TSKgel SuperAW4000) (Tosoh, Tokyo) controlled with GPC-8020 model II ver. 5.0 (Tosoh). A calibration curve was obtained using

poly(ethylene glycol) standards. The flow rate was 1.0 mL/min. The mobile phase was DMF containing 50 mmol/L LiCl, and the column temperature was controlled at 45 °C using a equipped column oven, and the elution profiles were monitored by a equipped refractometer.

XPS Analysis of Initiaotor-and PIPAAm modified Surfaces

Elemental analysis was performed for both ATRP-initiator modified and PIPAAm-brush grafted glass cover slips by an X-ray photoelectron spectroscope (XPS) (K-Alpha, Thermo Fisher Scientific, Waltham, MA). Excitation X-rays were produced from a monochromatic Al $K\alpha_{1,2}$ source and a take-off angle of 90°. Wide scans were recorded to analyze all existing elements on the surface, and high resolution narrow scan analysis was performed for the peak deconvolution of carbon C1s signals. All binding energies were referenced to a C1s hydrocarbon peak at 285.0 eV.

Amount of PIPAAm on Glass Substrates

Amount of grafted PIPAAm was determined by an attenuated total reflection Fourier transform infrared spectroscope (ATR/FT-IR) (Nicolet 6700) (Thermo Fisher Scientific) using germanium as an ATR crystal. Glass as the base substrate showed a strong absorption arising from Si–O at 1000 cm^{-1}. Absorption of amide carbonyl derived from PIPAAm appeared in the region of 1650 cm^{-1}. The peak intensity ratio of I_{1650} / I_{1000} was used to determine the amount of PIPAAm grafted surface using a calibration curve prepared from a series of known amounts of PIPAAm casts on unmodified glass surfaces. (The calibration curve and the detailed methods for measurement were shown in supplementary materials). Prepared glass coverslips were abbreviated as IP-x where x represent the grafted amount of PIPAAm on glass substrate.

Phase transition of PIPAAm in cell culture medium

Phase transitions of PIPAAm in cell culture mediums were observed through their optical transmittance changes. Solutions of PIPAAm with various molecular weights were prepared using

four different cell culture mediums; endothelial cell medium (EGM-2), fibroblast cell medium (FGM-2), smooth muscle cell medium (SmGM), and skeletal muscle cell medium (SkGM), and water (10 mg/mL). Optical transmittance changes of the polymer solutions were monitored at 600 nm with a UV-Vis spectrometer (V-660, JASCO, Tokyo). The sample cuvette was thermostated with a Peltier-effect cell holder (ETC-717, JASCO) with a heating rate of 0.10 °C/min. The lower critical solution temperature (LCST) of PIPAAm was defined as the temperature at 50% transmittance of solution.

Cell Culture and Cell Adhesion Behavior

Four types of cells, utilized for fabricating cell sheets on tissue, were used for investigating cells adhesion and detachment properties from the prepared surfaces. Human umbilical vein endothelial cells (HUVEC),[33, 34] normal human dermal fibroblasts (NHDF),[34-36] _ENREF_28 human aortic smooth muscle cells (SMC),[37-39] _ENREF_29 and human skeletal muscle myoblast cells (HSMM)[3, 40, 41] were cultured on conventional TCPS dishes (Becton, Dickinson and Company, Franklin Lakes) with endothelial cell medium (EGM-2), fibroblast cell medium (FGM-2), smooth muscle cell medium (SmGM), and skeletal muscle myoblast cell medium (SkGM), respectively. Cells were recovered from conventional TCPS dishes by treating with 0.1% trypsin containing 1.1 mmol/L EDTA in phosphate buffered saline (PBS). Recovered single cells were seeded on the prepared PIPAAm brush surfaces (coverslips) at 2.5 x 10^4 cells/mL to observing their adhesion and detachment. Cell suspensions were put on PIPAAm brush surfaces, which were incubated at 37 °C in a humidified atmosphere of 5% CO_2 for 24 h, then transferred to another incubator set at 20 °C, and again incubated for 4 h for observing both cell adhesion and detachment. Cell morphology was also photographed at predetermined time by a phase-contrast microscope (ECLIPSE TE2000-U) (Nikon, Tokyo) equipped with a digital camera (OXM1200C) (Nikon, Tokyo). GFP-HUVEC was photographed by a fluorescence microscope (ECLIPSE TE2000-U) equipped with a digital camera (AxioCam HRc, Carl ZEISS, Oberkochen, Germany) for observing the adhesion of GFP-HUVEC. Adhered cells were counted randomly on the

microphotographs in multiple areas. Percent cell adhesion was then calculated as the mean of four measurements with SD.

Results and discussion

Characterization of PIPAAm brush grafted glass surfaces

For investigating the elemental composition of the prepared surface, XPS measurement was performed. Table 1 summarizes the elemental compositions of the prepared surfaces, and Fig. 2 shows the peak deconvolution of XPS carbon C1s peaks the ATRP-initiator-modified surface and PIPAAm grafted glass surfaces. All samples were named with the abbreviated name of IPAAm, "IP", and the feed monomer concentration of IPAAm in ATRP. For example, PIPAAm brush grafted glass coverslip prepared by ATRP using 500 mmol/L IPAAm solution was named IP-500. In the spectrum of PIPAAm grafted glass surfaces (Fig. 2 (B)-(D)), an additional peak was observed at higher binding energy region, corresponding to the C=O bond of PIPAAm, while there was no peak in the spectrum of ATRP-initiator-modified glass slide (Fg.2(A)). These results indicated that PIPAAm was successfully grafted on glass surfaces through a surface-initiated ATRP. Additionally, in carbon and nitrogen contents increased, and silicon and oxygen contents decreased with increasing the grafted amount of PIPAAm, because PIPAAm brush layer thickness on the glass surfaces increased with proceeding ATRP reaction. This indicated that PIPAAm brush layer was unable to allow the chemical components of the base surface to be detected. In addition, the chlorine composition also decreased with ATRP reaction time. This was attributed to a poor photoelectron accessibility to the structure during XPS analysis, because chlorine was buried in PIPAAm layer, or lost during the termination reaction of radical coupling.[42]

Characterization of PIPAAm brush grafted surfaces by changing feed monomer concentration was summarized in Table 2. Amounts of grafted PIPAAm on glass surfaces, determined by ATR/FT-IR, were increased with increasing IPAAm monomer. Similarly, the molecular weight of prepared PIPAAm in reaction solution increased with increasing feed monomer concentration,

indicating that PIPAAm brush length increased with increasing feed monomer concentration, because a previous report indicates that the molecular weight of polymer in solution is expected to be similar to that of grafted polymer on substrate.[43] Polydispersity index of prepared PIPAAms in reaction solution was slightly larger compared to that of a polymer prepared by polymerization only in solution without grafting substrate, as previously reported.[44] This was attributed to the relatively smaller Cu^{II} complex in ATRP reaction. In our previous works for grafting PIPAAm on substrate through a surface-initiated ATRP, our laboratory used $CuCl_2$ for controlling polymerization in previous works,[28, 31] because the addition of $CuCl_2$ increases the Cu^{II} complex in reaction solution, leading to a controlled polymerization.[45] Similarly, previous reports regarding grafting polymer onto substrate via surface-initiated ATRP indicated that the addition of unbounded-initiator (free initiator) into ATRP reaction solution at the same time on grafting polymer onto substrate promotes to control polymerization, because the unbounded initiator increases the Cu^{II} complex, resulted in the control of polymerization.[45] In the present study, although the polymerization was controlled by some extent in the present ATRP, increase in free initiator or additional $CuCl_2$ was required for more controlled polymerization.

Estimated graft density exhibited a relatively higher value (> 0.1 chains/nm^2), indicating that ATRP reaction formed densely packed PIPAAm brush on glass substrates.[46] The dense PIPAAm brush structure was speculated to suppress an undetachable cell adhesion and other extracellular proteins adsorption on the glass substrate.

Phase transition behavior of PIPAAm with various lengths was investigated using cell culture medium, because the phase transition behavior of PIPAAm is known to be influenced by ion concentration[47] and molecular length.[48] Fig. 3 (A)-(C) shows the phase transition behavior of PIPAAm in cell culture medium. Table 3 summarized the phase transition temperature of PIPAAm in cell culture medium. Phase transition temperature slightly decreased with increasing molecular weight, which was consistent with the previous reports regarding the thermal response of narrow-disperse PIPAAm prepared by an atom transfer radical polymerization.[48, 49] Also, a smaller decrease in phase

transition temperatures was found compared to that in Milli-Q water by approximately 3 °C. This was attributed to a salting out effect[47] induced by salt in cell culture mediums. The phase transition temperatures of individual conditions were found between 20 °C and 37 °C, which were cell detachment and attachment temperatures, respectively.[50] These temperatures were adequate for cell-adhesion on 37 °C and detachment of 20 °C.

Cells adhesion on and detachment from intelligent-interfaces

Prepared PIPAAm brush surfaces with various brush lengths were evaluated as a thermo-responsive cell separating interface by observing the adhesion and detachment behavior of four different types of cells. Figs. 4-6 show the cell morphologies on prepared-PIPAAm-brush-grafted surfaces, and Fig. 7 shows cell-adhesion and detachment profiles on the prepared surfaces. On IP-500 surface, prepared by grafting short brush length, almost all cells adhered after 24 h incubation at 37 °C (Fig.4. (A-1), (B-1), (C-1), and (D-1)), indicating that the surface had a strong cell adhesive property. However, after incubation at 20 °C, SMC and HSMM scarcely detached themselves from the surface, approximately half amounts of HUVEC and NHDF detached from the surface (Fig.7 (A)). These cell-adhesive properties were attributed to the properties of short PIPAAm brush on substrate. Densely packed PIPAAm brush exhibited a relatively hydrophobic property compared to that of sparsely grafted PIPAAm brush, because of its low molecular mobility and a possible interaction among grafted polymer molecules.[29, 51, 52] Thus, cells tented to adhere on the short PIPAAm brush surface at 37 °C and scarcely detached from the surface. Additionally, the detachment rate of HUVEC was slightly higher than that of NHDF, which was probably due to the difference cell detachment properties from PIPAAm brush surface between HUVEC and NHDF.

Fig. 5 shows the cell morphologies on IP-875 surface, prepared by grafting a moderate length of PIPAAm on surface. After 37 °C incubation, all types of cells adhered on the surface. However, cell adhesion ratios on IP-875 were relatively low compared to those of IP-500, because longer PIPAAm brush was grafted on IP-875 substrate compared to that on IP-500. Our previous report

indicates that longer PIPAAm brush tend to hydrate compared to short PIPAAm brush because of its increased chain mobility.[52, 53] This properties affected the moderate adhesive properties of IP-875. After incubation at 20 °C, the larger ratio of cells detached from the surface compared to IP-500, because longer PIPAAm brush on IP-875 compared to that on IP-500 tends to hydrate and allow the adhered cells to detach more easily. Additionally, the detachment rate of HUVEC from IP-875 was higher than those of other cells. The difference in the detachment ratios among cells was speculated to be applicable to a good cell separation.

In IP-1000 surface, almost all cells scarcely adhered to the surfaces (Fig. 6), although the small amount of HSMM adhesion was observed. This was attributed to excessive long PIPAAm brush (Mn: 15600) on IP-1000 surface, leading to an unexpected higher hydrophilicity on the surface. Thus, this brush length was unable to modulate the on/off-adhesion of cells by external temperature change and inapplicable for cells separation.

These cell adhesion and detachment experiment results indicated that (1) an adequate cell adhesion and detachment on PIPAAm brush was obtained by grafting the moderate length of PIPAAm, approximately 12800 and (2) different cell detachment ratios were observed on the surfaces having various lengths of PIPAAm brush, while the adhesion rates of cells were almost the same. Utilizing these properties, the cell separation of HUVEC and HSMM, which have different detachment properties, was performed. GFP-expressing HUVEC was used in this separation for distinguishing individual cell adhesion and detachment properties. Mixed cells suspension consisting of GFP expressing HUVEC (GFP-HUVEC) and HSMM were seeded on IP-875 with EGM-2 as culture medium. Various other culture mediums were tested, such as Dulbecco's modified eagle medium (DMEM) and a mixture of EGM-2 and SkGM. However, effective cells adhesion on the surface was unable to be performed using these cells culture medium, probably due to the insufficient cellular adhesion factor in these cells culture medium. Thus, EGM-2 was found to be an appropriate cell culture medium for GFP-HUVEC and HSMM separation. Fig. 8 shows GFP-HUVEC and HSMM adhesion on and detachment from IP-875, and the cells morphologies on IP-875. Comparable adhesion behavior of two cells was

observed on IP-875, except that the adhesion ratio of HUVEC was slightly lower than that of individually incubated HUVEC on the surface (Figs. 4 and 7), probably due to the occupation of adhered HSMM on the surface. After incubation at 20 °C, almost all GFP-HUVEC promptly detached themselves from the surfaces, while almost all HSMM was able to adhere for the initial period. After subsequent incubation at 20 °C, adhered HSMM gradually detached from the surface. Thus, the high ratio of GFP-HUVEC was able to be recovered in medium at the initial period of incubation at 20 °C, and then subsequent incubation provided the high ratio of HSMM in medium. These results indicated that the precisely designed PIPAAm brush, prepared through the surface-initiated ATRP, was able to separate the mixture of cells by only changing external temperature.

Thus, the PIPAAm brush surfaces would be applicable to cell separation by utilizing the different cells detachment rates. The prepared surfaces would be useful as cell separation chromatography matrices or application to other cell separating devices, such as fields flow fractionation (FFF) or microfluidics.[54, 55] These prompts will be reported in the near future.

Conclusions

Dense PIPAAm brushes having various brush lengths were grafted onto glass surfaces, and these prepared surfaces were utilized for cell separation. Length of PIPAAm brush on glass substrate was adjusted by changing feed monomer concentration in a surface-initiated ATRP. On short PIPAAm brush grafted surface on glass, four types of human cells adhered with comparable adhesion rates. However, the recovery rates of adhered cells were relatively low, because the hydration of grafted short PIPAAm brush was insufficient for cell detachment. On the contrary, long PIPAAm brush grafted surface, almost all cells were unable to adhere, because the relatively higher hydrophilic PIPAAm brush suppressed the adhesion of these cells. On IP-875, prepared by grafting moderate brush length of PIPAAm, four types of cells were able to adhere and detach themselves after incubation at 20 °C. Using IP-875, a mixture of GFP-HUVEC and HSMM was allowed to adhere on the surface at 37 °C,

and then to be recovered at 20 °C. GFP-HUVEC detached from the surfaces promptly at initial incubation at 20 °C, and then HSMM gradually detached, indicating that the high ratio of HUVEC and HSMM were obtained in the initial and subsequent periods of 20 °C incubation, respectively. Thus, precisely designed PIPAAm brush was able to separate cells by the utilization of different detachment properties of cells from the surfaces.

Acknowledgement

Part of the present research was financially supported by the "Funding Program for World-Leading Innovative R&D on Science and Technology (FIRST Program)," initiated by the Council for Science and Technology Policy from the Japan Society for the Promotion of Science (JSPS). We would appreciate to Ms. Yuri Hatakeyama for preparing calibration curve, and Dr. Norio Ueno for English editing.

† ***Electronic supplementary information (ESI) available***:. Standard curve for estimating amount of grafted PIPAAm.

REFERENCES

1. P. Menasché, A. A. Hagège, M. Scorsin, B. Pouzet, M. Desnos, D. Duboc, K. Schwartz, J.-T. Vilquin and J.-P. Marolleau, *The Lancet*, 2001, **357**, 279-280.
2. K. Nishida, M. Yamato, Y. Hayashida, K. Watanabe, K. Yamamoto, E. Adachi, S. Nagai, A. Kikuchi, N. Maeda, H. Watanabe, T. Okano and Y. Tano, *N. Engl. J. Med.*, 2004, **351**, 1187-1196.
3. Y. Sawa, S. Miyagawa, T. Sakaguchi, T. Fujita, A. Matsuyama, A. Saito, T. Shimizu and T. Okano, *Surg. Today*, 2012, **42**, 181-184.

4. M. Hofmann, K. C. Wollert, G. P. Meyer, A. Menke, L. Arseniev, B. Hertenstein, A. Ganser, W. H. Knapp and H. Drexler, *Circulation*, 2005, **111**, 2198-2202.

5. H. Sekine, T. Shimizu, I. Dobashi, K. Matsuura, N. Hagiwara, M. Takahashi, E. Kobayashi, M. Yamato and T. Okano, *Tissue Engineering Part A*, 2011, **17**, 2973-2980.

6. R. Langer and J. Vacanti, *Science*, 1993, **260**, 920-926.

7. T. Shinoka and C. Breuer, *Yale J. Biol. Med.*, 2008, **81**, 161-166.

8. N. Yamada, T. Okano, H. Sakai, F. Karikusa, Y. Sawasaki and Y. Sakurai, *Makromol. Chem., Rapid Commun.*, 1990, **11**, 571-576.

9. M. Yamato, Y. Akiyama, J. Kobayashi, J. Yang, A. Kikuchi and T. Okano, *Prog. Polym. Sci.*, 2007, **32**, 1123-1133.

10. M. Heskins and J. E. Guillet, *J. Macromol. Sci. A*, 1968, **2**, 1441-1455.

11. K. Itoga and T. Okano, *J. Mater. Chem.*, 2010, **20**, 8768-8775.

12. T. Ohki, M. Yamato, D. Murakami, R. Takagi, J. Yang, H. Namiki, T. Okano and K. Takasaki, *Gut*, 2006, **55**, 1704-1710.

13. M. Kanzaki, M. Yamato, J. Yang, H. Sekine, C. Kohno, R. Takagi, H. Hatakeyama, T. Isaka, T. Okano and T. Onuki, *Biomaterials*, 2007, **28**, 4294-4302.

14. T. Iwata, M. Yamato, H. Tsuchioka, R. Takagi, S. Mukobata, K. Washio, T. Okano and I. Ishikawa, *Biomaterials*, 2009, **30**, 2716-2723.

15. K. Ohashi, T. Yokoyama, M. Yamato, H. Kuge, H. Kanehiro, M. Tsutsumi, T. Amanuma, H. Iwata, J. Yang, T. Okano and Y. Nakajima, *Nat. Med.*, 2007, **13**, 880-885.

16. K. Matsuura, S. Masuda, Y. Haraguchi, N. Yasuda, T. Shimizu, N. Hagiwara, P. W. Zandstra and T. Okano, *Biomaterials*, 2011, **32**, 7355-7362.

17. S. Sekiya, T. Shimizu, M. Yamato, A. Kikuchi and T. Okano, *Biochem. Biophys. Res. Commun.*, 2006, **341**, 573-582.

18. J. C. Giddings, N. Barman Bhajendra and M.-K. Liu, in *Cell Separation Science and Technology*, American Chemical Society, 1991, pp. 128-144.

19. T. Chianéa, N. E. Assidjo and P. J. P. Cardot, *Talanta*, 2000, **51**, 835-847.

20. K. Kataoka, in *Cell Separation Science and Technology*, American Chemical Society, 1991, pp. 159-174.

21. K. Kataoka, Y. Sakurai, T. Hanai, A. Maruyama and T. Tsuruta, *Biomaterials*, 1988, **9**, 218-224.

22. A. Moldavan, *Science*, 1934, **80**, 188-189.

23. F. Leary James, P. Ellis Steven, R. McLaughlin Scott, A. Corio Mark, S. Hespelt, G. Gram Janet and S. Burde, in *Cell Separation Science and Technology*, American Chemical Society, 1991, pp. 26-40.

24. L. A. Herzenberg and L. A. Herzenberg, in *Handbook of Experimental Immunology*, ed. D. M. Weir, Blackwell Scientific Publication, Oxford, 1978, pp. 22.21-22.21.

25. Y. Akiyama, A. Kikuchi, M. Yamato and T. Okano, *Langmuir*, 2004, **20**, 5506-5511.

26. T. Yakushiji, K. Sakai, A. Kikuchi, T. Aoyagi, Y. Sakurai and T. Okano, *Langmuir*, 1998, **14**, 4657-4662.

27. H. Takahashi, M. Nakayama, M. Yamato and T. Okano, *Biomacromolecules*, 2010, **11**, 1991-1999.

28. K. Nagase, M. Watanabe, A. Kikuchi, M. Yamato and T. Okano, *Macromol. Biosci.*, 2011, **11**, 400-409.

29. K. Nagase, J. Kobayashi, A. Kikuchi, Y. Akiyama, H. Kanazawa and T. Okano, *Langmuir*, 2007, **23**, 9409-9415.

30. K. Nagase, S. F. Yuk, J. Kobayashi, A. Kikuchi, Y. Akiyama, H. Kanazawa and T. Okano, *J. Mater. Chem.*, 2011, **21**, 2590-2593.

31. K. Nagase, J. Kobayashi, A. Kikuchi, Y. Akiyama, H. Kanazawa and T. Okano, *Langmuir*, 2008, **24**, 511-517.

32. M. Ciampolini and N. Nardi, *Inorg. Chem.*, 1966, **5**, 41-44.

33. T. Sasagawa, T. Shimizu, S. Sekiya, Y. Haraguchi, M. Yamato, Y. Sawa and T. Okano, *Biomaterials*, 2010, **31**, 1646-1654.

34. N. Asakawa, T. Shimizu, Y. Tsuda, S. Sekiya, T. Sasagawa, M. Yamato, F. Fukai and T. Okano, *Biomaterials*, 2010, **31**, 3903-3909.

35. H. Kobayashi, T. Shimizu, M. Yamato, K. Tono, H. Masuda, T. Asahara, H. Kasanuki and T. Okano, *J. Artificial Organs*, 2008, **11**, 141-147.

36. Y. Tsuda, T. Shimizu, M. Yamato, A. Kikuchi, T. Sasagawa, S. Sekiya, J. Kobayashi, G. Chen and T. Okano, *Biomaterials*, 2007, **28**, 4939-4946.

37. K. Hobo, T. Shimizu, H. Sekine, T. Shin'oka, T. Okano and H. Kurosawa, *Arterioscler. Thromb. Vasc. Biol.*, 2008, **28**, 637-643.

38. H. Takahashi, N. Matsuzaka, M. Nakayama, A. Kikuchi, M. Yamato and T. Okano, *Biomacromolecules*, 2011.

39. B. C. Isenberg, Y. Tsuda, C. Williams, T. Shimizu, M. Yamato, T. Okano and J. Y. Wong, *Biomaterials*, 2008, **29**, 2565-2572.

40. H. Kondoh, Y. Sawa, S. Miyagawa, S. Sakakida-Kitagawa, I. A. Memon, N. Kawaguchi, N. Matsuura, T. Shimizu, T. Okano and H. Matsuda, *Cardiovasc. Res.*, 2006, **69**, 466-475.

41. H. Hata, G. Matsumiya, S. Miyagawa, H. Kondoh, N. Kawaguchi, N. Matsuura, T. Shimizu, T. Okano, H. Matsuda and Y. Sawa, *J. Thorac. Cardiovasc. Surg.*, 2006, **132**, 918-924.

42. D. Xiao and M. J. Wirth, *Macromolecules*, 2002, **35**, 2919-2925.

43. K. Ohno, K.-m. Koh, Y. Tsujii and T. Fukuda, *Macromolecules*, 2002, **35**, 8989-8993.

44. K. Nagase, A. Mizutani Akimoto, J. Kobayashi, A. Kikuchi, Y. Akiyama, H. Kanazawa and T. Okano, *J. Chromatogr. A*, 2011, **1218**, 8617-8628.

45. M. Ejaz, S. Yamamoto, K. Ohno, Y. Tsujii and T. Fukuda, *Macromolecules*, 1998, **31**, 5934-5936.

46. T. Wu, K. Efimenko and J. Genzer, *J. Am. Chem. Soc.*, 2002, **124**, 9394-9395.

47. T. G. Park and A. S. Hoffman, *Macromolecules*, 1993, **26**, 5045-5048.

48. Y. Xia, X. Yin, N. A. D. Burke and H. D. H. Stover, *Macromolecules*, 2005, **38**, 5937-5943.

49. Y. Xia, N. A. D. Burke and H. D. H. Stöver, *Macromolecules*, 2006, **39**, 2275-2283.

50. T. Okano, N. Yamada, M. Okuhara, H. Sakai and Y. Sakurai, *Biomaterials*, 1995, **16**, 297-303.

51. K. Nagase, J. Kobayashi, A. Kikuchi, Y. Akiyama, M. Annaka, H. Kanazawa and T. Okano, *Langmuir*, 2008, **24**, 10981-10987.

52. Y. Hattori, K. Nagase, J. Kobayashi, A. Kikuchi, Y. Akiyama, H. Kanazawa and T. Okano, *Chem. Phys. Lett.*, 2010, **491**, 193-198.

53. A. Mizutani, A. Kikuchi, M. Yamato, H. Kanazawa and T. Okano, *Biomaterials*, 2008, **29**, 2073-2081.

54. J. C. Bigelow, J. C. Giddings, Y. Nabeshima, T. Tsuruta, K. Kataoka, T. Okano, N. Yui and Y. Sakurai, *J. Immunol. Methods*, 1989, **117**, 289-293.

55. A. Kikuchi, M. Karasawa, T. Tsuruta and K. Kataoka, *J. Colloid Interface Sci.*, 1993, **158**, 10-18.

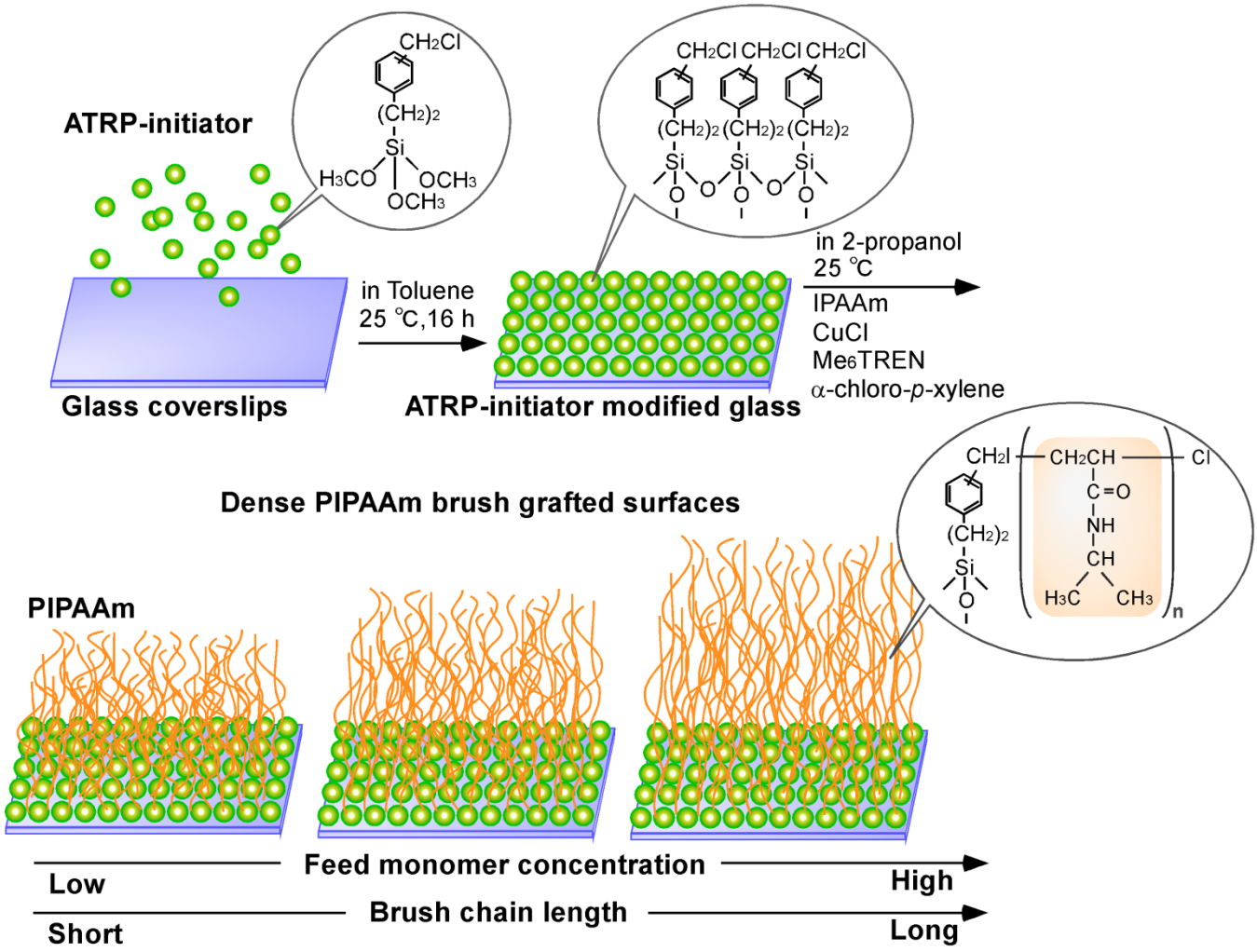

Fig. 1 Scheme of the preparation of poly(*N*-isopropylacrylamide) (PIPAAm) brush grafted glass surface as an intelligent biointerface for cell separation.

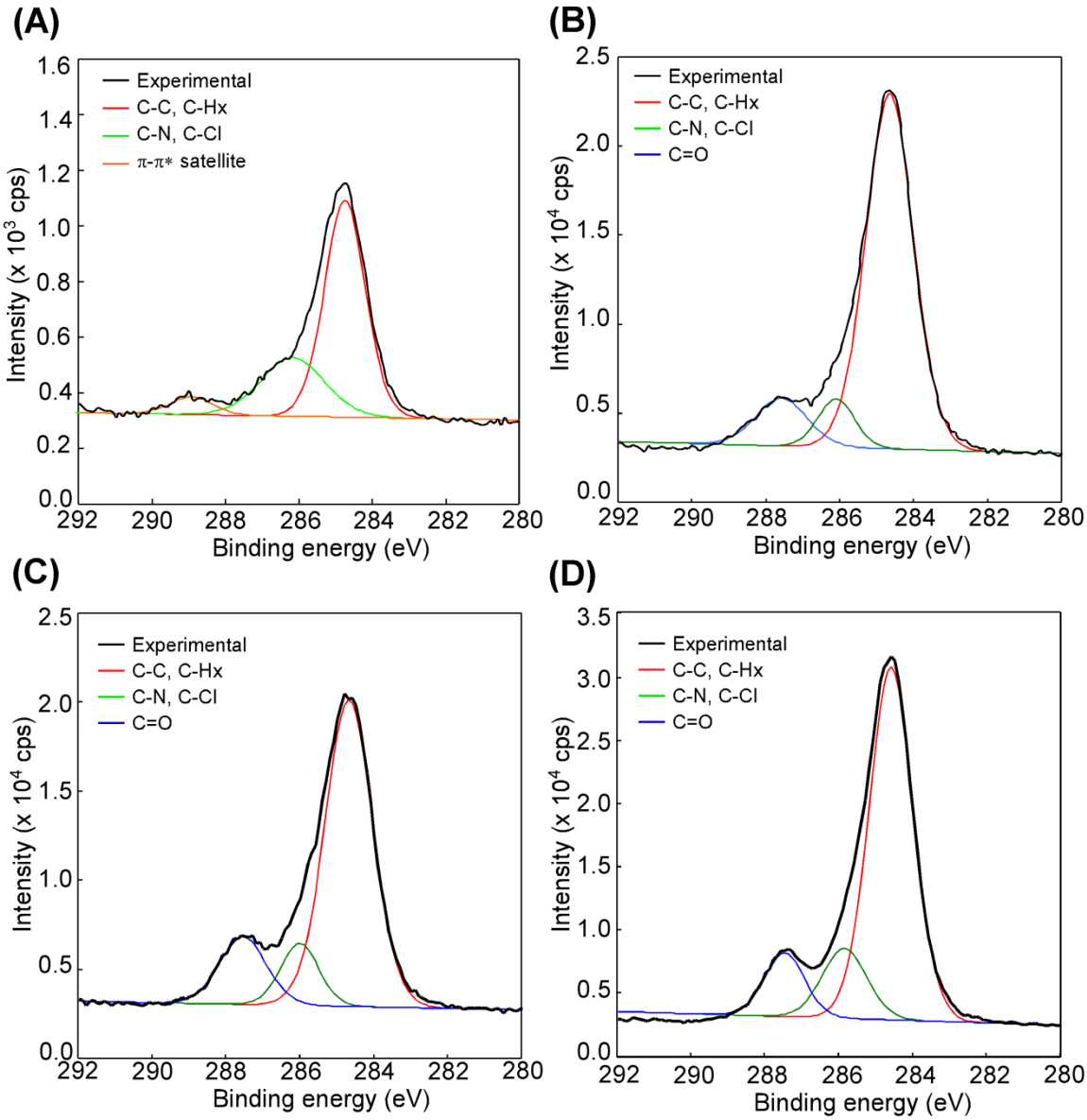

Fig. 2 Peak deconvolution of XPS C1s peaks for (A) Initiator modified glass surface, (B) short poly(*N*-isopropylacrylamide)(PIPAAm) brush grafted surface (IP-500), (C) moderate PIPAAm brush grafted surface (IP-875), and (D) long PIPAAm brush grafted surface (IP-1000). All sample surfaces were abbreviated as IP-X, where X is feed monomer concentration in ATRP (Table 2).

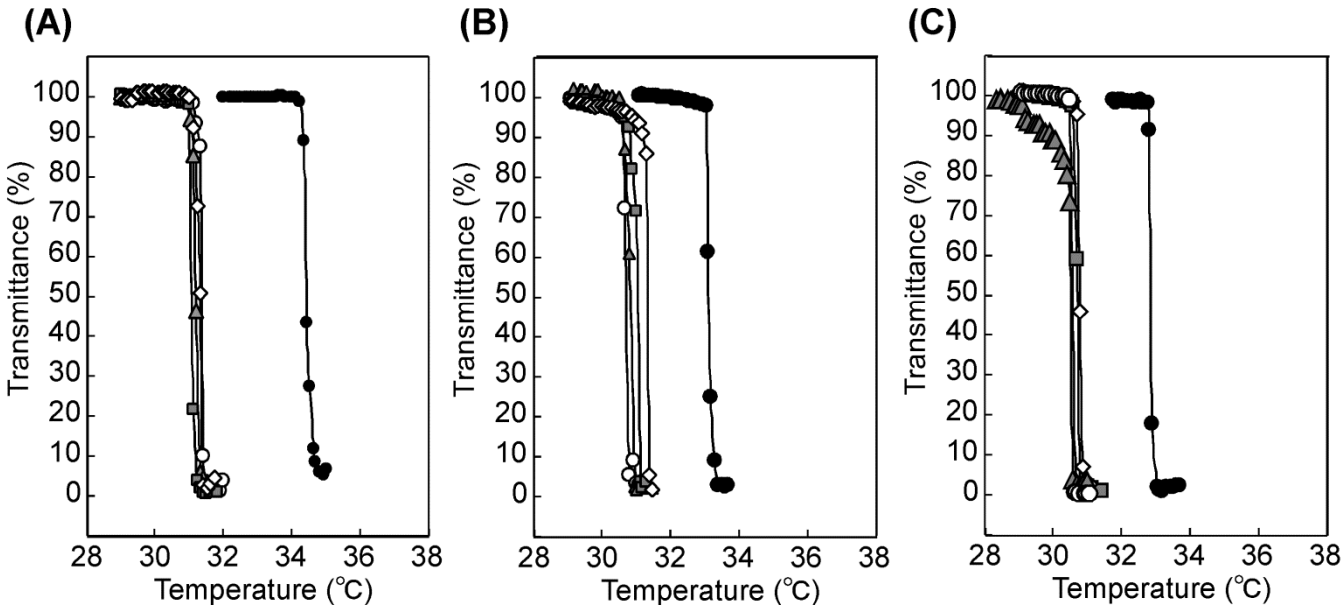

Fig. 3 Phase transition profiles of unbounded poly(*N*-isopropylacrylamide)(PIPAAm) (A) short PIPAAm brush grafted surface (IP-500), (B) moderate PIPAAm brush grafted surface (IP-875), and (C) long PIPAAm brush grafted surface (IP-1000) in various cell culture mediums. The closed circles represent transition in water; the open circles, endothelial cell medium (EGM-2); the closed triangles, fibroblast cell medium (FGM-2); the open diamonds, smooth muscle myoblast cell medium (SmGM); and the closed squares, skeletal muscle cell medium (SkGM). All sample surfaces were abbreviated as IP-X, where X is feed monomer concentration in ATRP (Table 2).

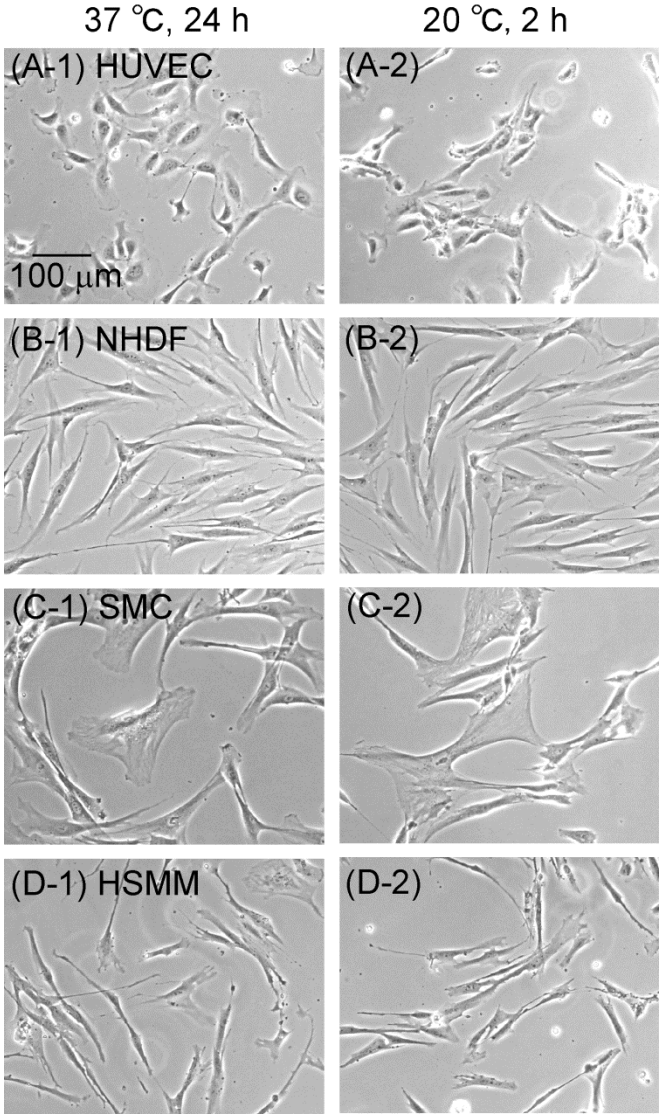

Fig. 4 Cell morphologies on short poly(*N*-isopropylacrylamide)(PIPAAm) brush grafted surface (IP-500): (A) human umbilical vein endothelial cells (HUVEC), (B) normal human dermal fibroblasts (NHDF), (C) human aortic smooth muscle cells (SMC), and (D) human skeletal muscle myoblast cells (HSMM). Cell morphologies at 37 °C and 20 °C were observed after 24 h and 2 h incubations, respectively.

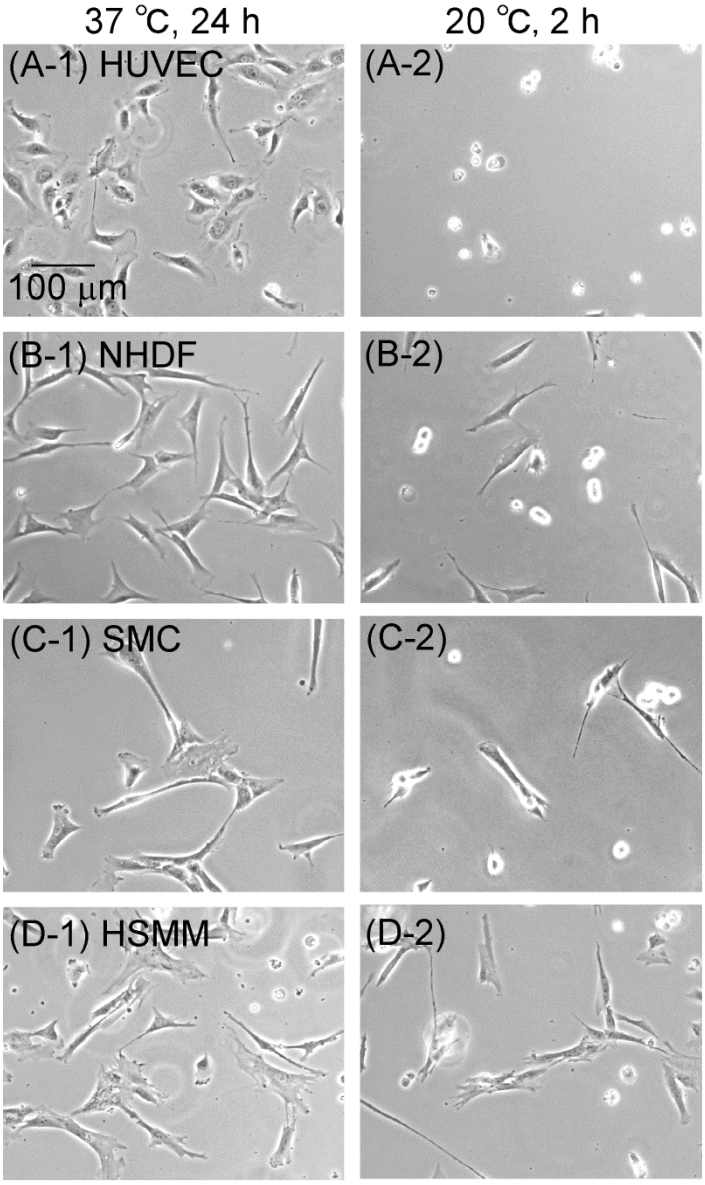

Fig. 5 Cell morphologies on moderate poly(*N*-isopropylacrylamide)(PIPAAm) brush grafted surface (IP-875): (A) human umbilical vein endothelial cells (HUVEC), (B) normal human dermal fibroblasts (NHDF), (C) human aortic smooth muscle cells (SMC), and (D) human skeletal muscle myoblast cells (HSMM). Cell morphologies at 37 °C and 20 °C were observed after 24 h and 2 h incubations, respectively.

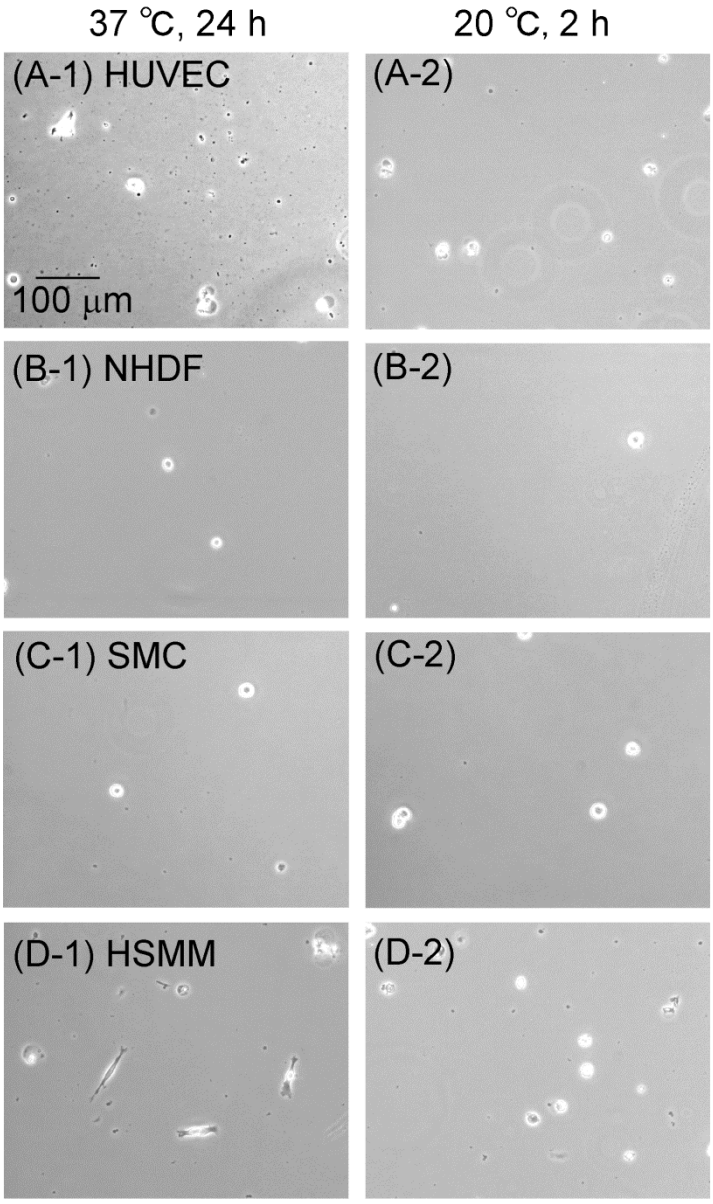

Fig. 6 Cell morphologies on long poly(*N*-isopropylacrylamide)(PIPAAm) brush grafted surface (IP-1000): (A) human umbilical vein endothelial cells (HUVEC), (B) normal human dermal fibroblasts (NHDF), (C) human aortic smooth muscle cells (SMC), and (D) human skeletal muscle myoblast cells (HSMM). Cell morphologies at 37 °C and 20 °C were observed after 24 h and 2 h incubations, respectively.

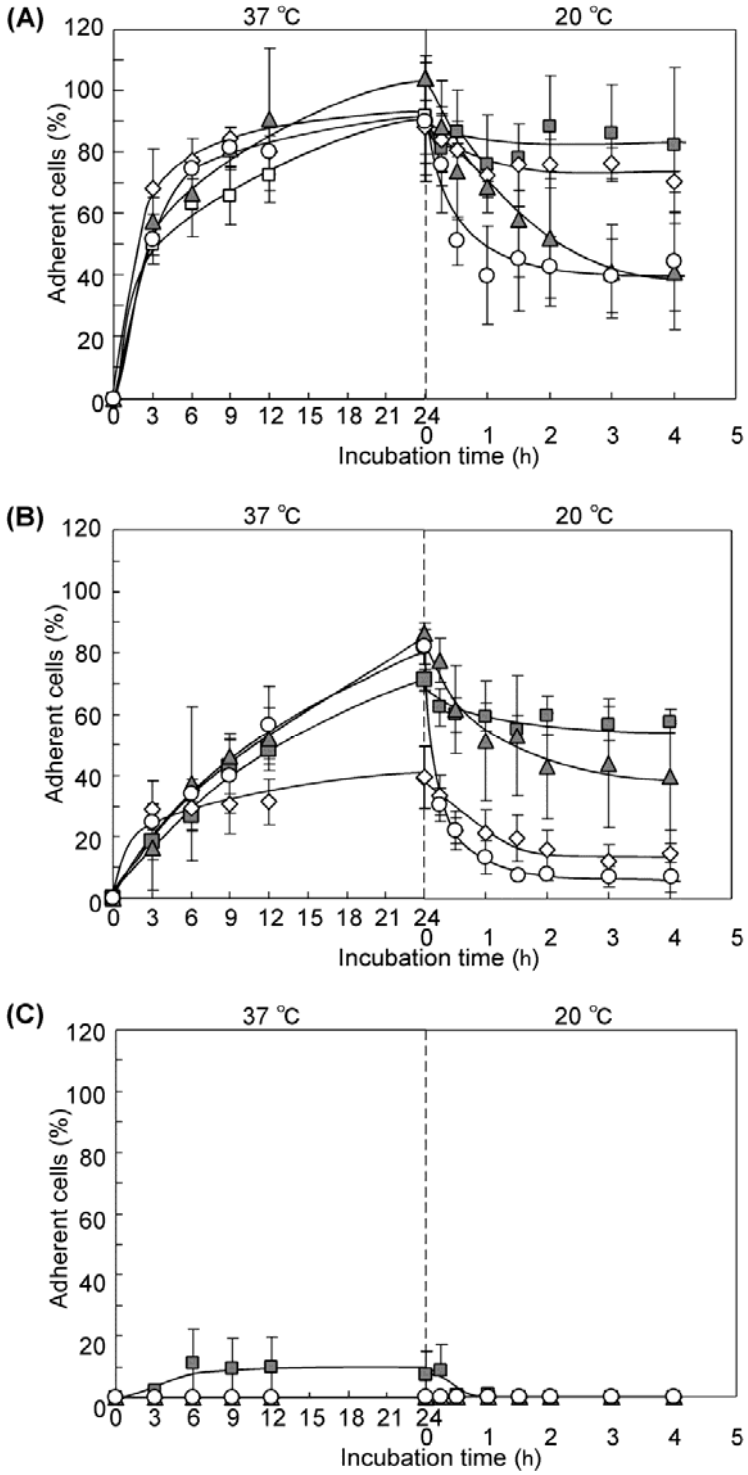

Fig. 7 Cells adhesion on and detachment from (A) short PIPAAm brush grafted surface (IP-500), (B) moderate PIPAAm brush grafted surface (IP-875), and (C) long PIPAAm brush grafted surface (IP-1000) in each cell culture medium. The open circles represent human umbilical vein endothelial cells (HUVEC); the closed triangles, normal human dermal fibroblasts (NHDF); the open diamonds, normal aortic smooth muscle cells (SMC); the closed squares, human skeletal muscle myoblast cells (HSMM). All sample surfaces were abbreviated as IP-X, where X is feed monomer concentration in ATRP (Table 2).

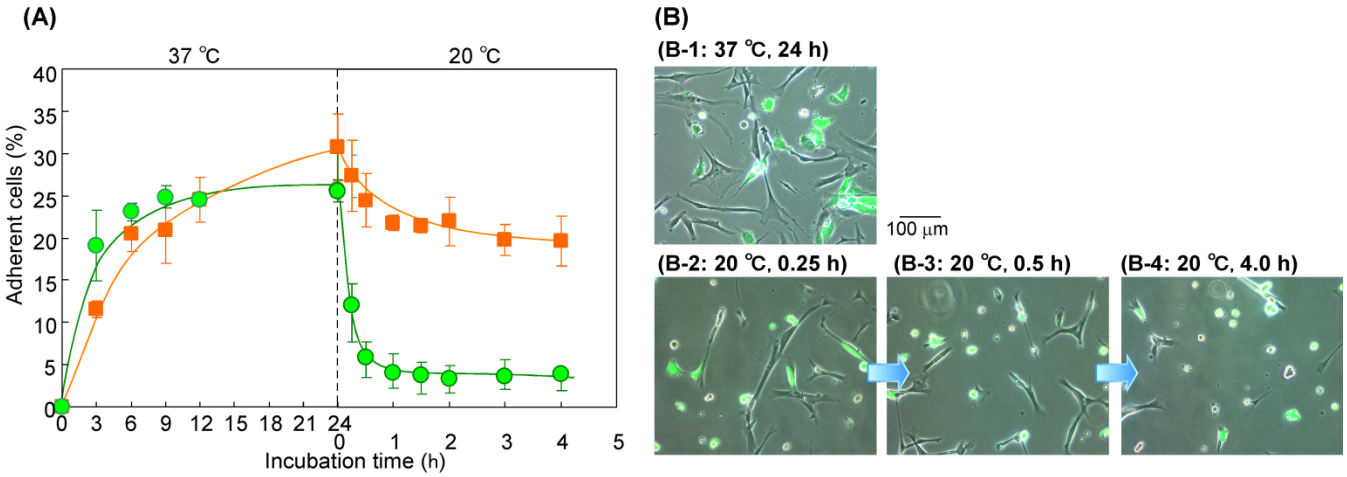

Fig. 8 (A) Cells adhesion on and detachment from moderate brush length poly(*N*-isopropylacrylamide)(PIPAAm) brush grafted surface (IP-875) in EGM-2. The green circles and the orange squares represent GFP expressing human umbilical vein endothelial cells (GFP-HUVEC) and human skeletal muscle myoblast cells (HSMM). (B) Cell morphologies on IP-875 (B-1) at 37 °C after 37 h incubation, (B-2) at 20 °C after 0.25 h, (B-3) at 20 °C after 0.5 h, and (B-4) at 20 °C after 4 h.

Table 1 Elemental analyses of poly(*N*-isopropylacrylamide)(PIPAAm) brush grafted glass surfaces by an X-ray photoelectron spectroscope (XPS) take-off angle of 90°

Code [a)]	IPAAm monomer concentration (mmol/L)	Atom (%)					N/C ratio
		C	N	O	Si	Cl	
Initiator modified glass		28.8	2.0	44.3	23.9	0.9	0.07
IP-500	500	58.1	6.5	22.4	12.3	0.7	0.11
IP-875	875	61.0	9.6	19.3	9.7	0.4	0.16
IP-1000	1000	73.8	10.6	13.4	1.8	0.3	0.14
Calcd [b)]		75.0	12.5	12.5	-	-	0.17

a) All samples were named using IPAAm monomer concentration in atom transfer radical polymerization (ATRP). b) Theoretical atomic composition of (*N*-isoporpylacrylamide) monomer.

Table 2 Characterization of poly(*N*-isopropylacrylamide)(PIPAAm) brush modified glass substrate

Code [a)]	IPAAm monomer concentration (mmol/L)	Amount of PIPAAm ($\mu g/cm^2$) [b)]	*Mn* [c)]	*Mn/Mw* [c)]	Grafted density (chains/nm^2)
IP-500	500	0.39 ± 0.38	8200	1.31	0.29
IP-875	875	0.76 ± 0.03	12800	1.27	0.36
IP-1000	1000	1.29 ± 0.18	15600	1.41	0.50

a) All samples were named using feed monomer concentration in atom transfer radical polymerization (ATRP). b) Determined by ATR/FT-IR measurement. c) Determined by GPC using DMF containing 50 mmol/L LiCl.

Table 3 Phase transition temperature of poly(*N*-isopropylacrylamide)(PIPAAm) in various cell culture mediums.

Code [a)]	IPAAm monomer concentration (mmol/L)	*Mn* [b)]	Phase transition temperature (°C) [c)]				
			Water	EGM-2	FGM-2	SmGM-2	SkGM-2
IP-500	500	8200	34.4	31.4	31.2	31.3	31.2
IP-875	875	12800	33.0	30.6	30.7	31.3	30.9
IP-1000	1000	15600	32.7	33.6	30.5	30.7	30.6

a) All samples were named using IPAAm monomer concentration in ATRP. b) Determined by GPC using DMF containing 50 mmol/L LiCl. c) Defined as temperature at 50% transmittance. d) EGM-2 represents endothelial cell medium; FGM-2, fibroblast cell medium; SmGM, smooth muscle cell medium; and SkGM, skeletal muscle myoblast cell medium.